IEEE Access
Multidisciplinary | Rapid Review | Open Access Journal

Received February 11, 2019, accepted February 19, 2019, date of publication February 25, 2019, date of current version March 20, 2019.

Digital Object Identifier 10.1109/ACCESS.2019.2901013

Improved Algorithm of Radar Pulse Repetition Interval Deinterleaving Based on Pulse Correlation

ZHIPENG GE[1,2,3], (Student Member, IEEE), XIAN SUN[1,2,3], WENJUAN REN[1,3], WENBIN CHEN[1,2,3], AND GUANGLUAN XU[1,3]

[1]Institute of Electronics, Chinese Academy of Science, Beijing 100190, China
[2]University of Chinese Academy of Science, Beijing 100049, China
[3]Key Laboratory of Network Information System Technology, Institute of Electronics, Chinese Academy of Science, Beijing 100190, China

Corresponding author: Xian Sun (sunxian@mail.ie.ac.cn)

This work was supported in part by the National Natural Science Foundation of China under Grant 61725105.

ABSTRACT In the electromagnetic space, a single channel radar receiver will often intercept several periodic pulse trains radiating from the surrounding emitters simultaneously. The aim of radar pulse deinterleaving is to sort out the pulses coming from different emitters. Most traditional pulse repetition interval (PRI) deinterleaving methods are easy to sort out the pulses with small PRI fluctuations but difficult in dealing with relatively bigger fluctuation or staggered PRIs. In addition, this searching procedure can easily cause pulse omission phenomenon and even generate false pulses. In this paper, we propose an improved histogram method for PRI deinterleaving based on pulse correlation to overcome the above-mentioned shortcomings. After calculating the multi-level time difference histogram, we introduce the mean filter and interquartile range algorithm to optimize the estimated PRI values. Our method extracts the pulse pairs based on pulse correlation directly instead of searching for the pulses and then determines whether the PRI is staggered or not. The experiments on simulation data show that our method can achieve better performance on both the pulse trains of jittered PRIs and the staggered PRIs.

INDEX TERMS Radar signal, pulse deinterleaving, pulse correlation, jittered PRI, staggered PRI.

I. INTRODUCTION

In the electronic warfare (EW), the electronic support measure (ESM) refers to collect radar and communication signals emanating from military platforms [1], [2]. Hence, it is necessary to improve the effectiveness of radar pulse deinterleaving, which is the precondition of further signal processing and emitter classification. In recent decades, the electromagnetic environment has become increasingly complicated because of continuously increasing number of radars and improved radar technology. The radar pulse deinterleaving faces many challenges, such as high density of signals in electromagnetic space, extreme complexity of signal parameters, low probability of signal interception and so on [3]. Correspondingly, the deinterleaving algorithm should be improved to adapt to the complicated electromagnetic environment. Generally, a parametric pulse description word (PDW) will be generated [4], [5] when a pulse signal is intercepted, which generally contains the time of arrival (TOA), radio frequency (RF), pulse width (PW), pulse amplitude (PA), and direction of arrival (DOA). Pre-deinterleaving with the last four parameters is to dilute the pulse stream and separate them into several subspaces. The following deinterleaving with TOA attempts to extract TOA trains according to different PRIs. Since 1980s, lots of PRI deinterleaving algorithms have been proposed. Rogers [6] began to study real-time signal sorting algorithms in dense complex signal environments based on TOAs. After that, many PRI deinterleaving algorithms sprang out. These algorithms that have been applied in the actual scene can be mainly divided into three categories: direct sequence searching, time-difference histogram and PRI transformation. The methods based on direct sequence searching [7], [8] firstly chose a base pulse, then operated expanding searching procedure and picked out the prescribed number of pulses. The same operation for the remaining pulses will be repeated after sorting out a pulse train. This kind of methods are difficult to deinterleave TOAs of the staggered PRI and cannot solve pulse-missing problems. Histogram methods,

The associate editor coordinating the review of this manuscript and approving it for publication was Weimin Huang.

like cumulative difference histogram(CDIF) [9] and sequential difference histogram(SDIF) [10], estimate PRIs from a cumulative histogram based on time-difference of arrival (TDOA), and then search the TOA train by the estimated PRIs. These methods are time consuming when the number of TOAs is huge and the searching procedure would cause the same problems like the direct sequence searching methods do. Many further improved algorithms based on SDIF have been proposed. For instance, Liu and Zhang [3] focused on missing pulses and estimated more precise PRI values. Besides, it turns out to be fast when the entire searching procedure is in a linear manner. Xi *et al*. [11] introduced the overlapping box and dynamic sequence search algorithm based on classic SDIF method, which could deinterleave the PRI-jittered signals with jitter quantity less than 10%. Meanwhile, Ken'ichi and Masaaki [12] proposed an approach named PRI transformation, and its improved versions [13], [14] were proposed later. PRI transformation adopted correlation of inter-pulse with a phase factor, which was good at eliminating the interference of sub-harmonics. However, PRI transformation requires huge calculation, which is not suitable for the TOA streams of high density. All deinterleaving algorithms mentioned above contain two main procedures: estimating PRI values and searching for the TOA trains corresponding to them. These kinds of algorithms can successfully sort out pulses formed by lightly-fluctuated PRIs. However, when the fluctuation of PRI is bigger, extracting pulse with the estimated PRIs will lead to time consuming and searching confliction. Also, these algorithms did not pay too much attention to the complicated PRI types like the staggered, so it is not robust for the increasingly complex electromagnetic environment.

Besides the three main categories of PRI deinterleaving methods, several other deinterleaving algorithms based on TOAs showed their advantages on specialized applicable scenes. Quan *et al*. [15] separated pulse signals from a multiple superposed pulse train in synchronized scene with small pulse missing rate and jitter rate. Ata'a and Abdullah [16] proposed a neural network called ART for clustering, which was applied in the processing system with other histogram methods. Li *et al*. [17] deinterleaved pulses based on pulse correlation. The method recorded the pulse indexes while calculating the cumulative TDOA histogram and replaced the search process with sorting out the TOA trains based on the records directly. This kind of method could achieve better performance in jittered PRIs than the methods with search process, but still did not do well in the pulse trains mixed of complicated PRIs, especially the staggered PRIs. Ren *et al*. [18] proposed a location method on multi-TDOA of three satellites, which transformed the TDOAs into location information and by which emitters could be sorted out in space domain. Xie *et al*. [19] searched and extracted the radar pulse signal according to the pulse similarity after calculating the PRI values. Such method still needed the searching procedure, the order of which would have a great influence on the performance. Yu *et al*. [20] presented a method based on the cumulative square sine wave interpolation to solve jittered signals, which also needed the searching procedure. From the above discussion of deinterleaving algorithms based on TOAs, we conclude that most of the methods attempted to search for the TOA trains with the estimated PRI values. However, even the estimated PRI values are precise, the searching procedure might fail due to the missing pulses, and the fluctuation of PRIs would cause the conflict in searching.

In this paper, we propose an improved histogram method based on pulse correlation. We reduce the histogram computational complexity from $\mathbf{O}(kn^2)$ to $\mathbf{O}(kn)$ compared with the traditional histogram methods. Furthermore, more precise PRI values are estimated by utilizing mean filter and IQR algorithm. Instead of searching for pulse sequence, we extract the pulses with higher recalling rate by pulse correlation. We also take the staggered PRIs into consideration. The main contributions are summarized as follows: 1) calculating the cumulative TDOA histogram once within a fixed level; 2) adopting a mean filter for TDOA histogram and IQR algorithm for PRI ranges to optimize the estimated the PRI values; 3) extracting the TOAs based on pulse correlation and adopting a strategy to process the staggered PRIs.

The rest of this paper is organized as follows. In Section II, the characteristics of different PRI types are introduced and the process of data simulation is described. Section III will introduce the details of the whole algorithm followed by a flow chart of the complete process. In Section IV, experimental results and comparison with other PRI interleaving algorithm will be demonstrated. Finally, conclusions will be drawn in Section V.

II. PRI MODELS AND DATA SIMULATION

A. MODELING OF DIFFERENT PRI TYPES

In this section, we mainly introduce the different PRI type models, including the fixed, jittered, sine-modulated, slippery and staggered tpyes. Since the pulse signal radiated by a specific radar emitter satisfies certain rule, the TOAs can be defined as:

$$TOA_n = TOA_{n-1} + PRI_{n-1}, \tag{1}$$

Here, n is the sequential number of TOAs and PRI_{n-1} represents the changing time difference between adjacent TOAs.

Fig.1 shows TOAs of pulses received by antenna from a specific emitter. Every current TOA is related to the previous TOA and current PRI. Meanwhile, the general PRI is in the range of $100\mu s \sim 10000\mu s$. When the radar radiates pulses at

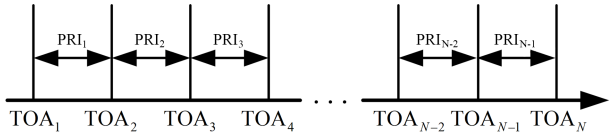

FIGURE 1. TOAs of pulses received by antenna from a specific emitter.

intervals of one PRI, the instantaneous PRIs can be formulated as:

$$PRI_n = PRI_0(1+\delta), \delta \in \left[-\frac{\delta_{max}}{2}, \frac{\delta_{max}}{2}\right] \quad (2)$$

Here, PRI_0 is the central value of PRIs and δ is the jitter rate of PRIs relative to PRI_0. The PRI can be regarded as fixed when δ is less than or equal to 0.01, and jittered when greater than 0.01 and less than 0.3 [4]. Furthermore, the radar emitter may perform specific types of modulation on the jittered PRIs. For example, formula (3) shows the sine modulation and formula (4) shows the slippery PRIs.

$$PRI_n = PRI_0\left[Rsin(2\pi vn + \varphi_0)\right] \quad (3)$$

$$PRI_n = PRI_0\left\{1 + \frac{2k}{M}\left[Mod(n, M) - \frac{M}{2}\right]\right\} \quad (4)$$

In formula (3), R represents the sine modulation ratio; v is the modulation frequency; φ_0 is the initial modulation phase. In formula (4), k is the slippery slope; n is the present time; M is slippery period; $Mod(\bullet)$ represents remainder operation.

A staggered PRI model can be represented as formula (5), where 'staggered' means radar emitters alternately radiate pulses outward at several fixed time intervals. Here, K is the number of sub PRIs, and sum of the K sub PRIs is called frame period.

$$PRI_n = PRI_{K_{Mod(n,K)}} \quad (5)$$

Fig.2 reveals that the radar radiates pulses at two intervals alternately. The TOA train can also be regarded as two pulse train from different emitters with the similar interval PRI_T. Consequently, it is difficult to sort out the pulses without other features in PDW. In our paper, we assume that all the emitters in simulation data do not share the same PRI(s).

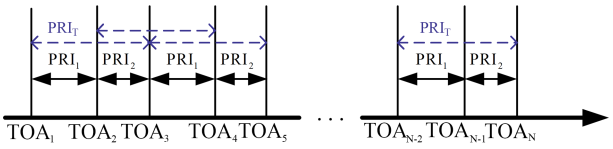

FIGURE 2. TOAs of pulses received from a specific emitter in which PRI is staggered with two PRIs.

B. DATA SIMULATION

On basis of the models mentioned in II-A, experimental TOA train within 0.5s is simulated. Table 1 lists the detailed parameters of simulation TOA trains. For short, Fix., Jit., Sta., Sin. and Slip. are adopted to represent fixed, jittered, staggered, sine modulated and slippery PRIs, respectively. In detail, 2% pulses are randomly dropped. Here, we show simulation data of the five PRI types in Fig.3.

Fig.3 shows that the PRIs of different PRI type change over the sampling time. PRIs of fixed type centered around $200\mu s$ fluctuate within a small range, while the jittered PRIs centered around $142\mu s$ have a wider fluctuation band. As for sine-modulated centered around $333\mu s$ and slippery centered around $500\mu s$ PRIs, they can be regarded as special cases of jittered PRIs. In the time domain, the staggered PRIs have two sub PRIs, shown in Fig.3, which are around $263\mu s$ and $286\mu s$, respectively. So the PRI deinterleaving algorithms are needed to sort out these pulses from different emitters.

TABLE 1. Simulation parameters of different PRI types.

PRI Type	PRI Values(μs)	Other parameters
Fix.	200	$\delta_{max} = 0.01$
Jit.	143	$\delta_{max} = 0.01$
Sin.	333	$R = 0.05, v = 50Hz, \delta_{max} = 0.01$
Slip.	500	$k = 0.05, M = 40, \delta_{max} = 0.01$
Sta.	263,286	$\delta_{max} = 0.01$

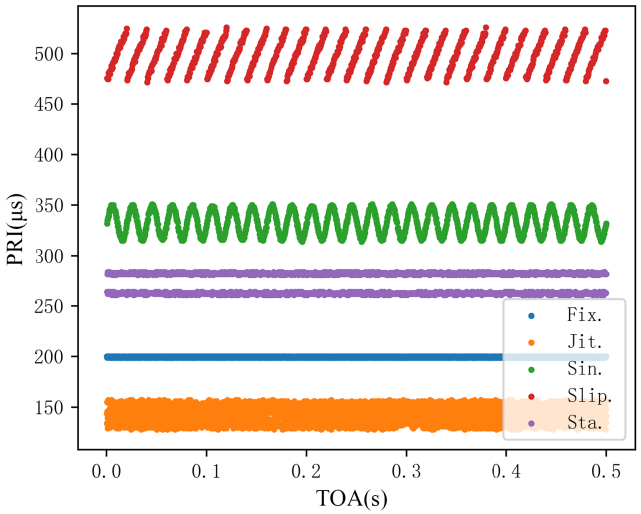

FIGURE 3. Instantaneous PRIs of different PRI type.

III. PRI DEINTERLEAVING BASED ON PULSE CORRELATION

A. FLOW CHART OF THE WHOLE ALGORITHM

We propose an algorithm which can handle the complicated situation when the PRIs are mixed with jittered and staggered types. Firstly, we calculate the multi-level TDOA histogram, and record the pulse pair indexes corresponding to time difference. Then we calculate the threshold by the mean-filtered histogram statistics. After that, the time differences where the relevant histogram statistics are beyond the threshold are obtained. Next, the possible PRIs with IQR are estimated and optimized. Finally, we extract the pulses according to the PRIs and optimize the results.

Fig.4 illustrates the flow chart for the whole algorithm. γ in Fig.4 is explained in Algorithm 2. To avoid redundant computation or false alarm caused by the noise, we use a mean filter to smooth the TDOA histogram distribution. After the comparison of the filtered histogram with the threshold, the raw estimated PRI ranges are obtained. Then the IQR algorithm [21] is adopted to optimize the estimated PRI values. Based on the optimal estimated PRIs, pulse indexes are

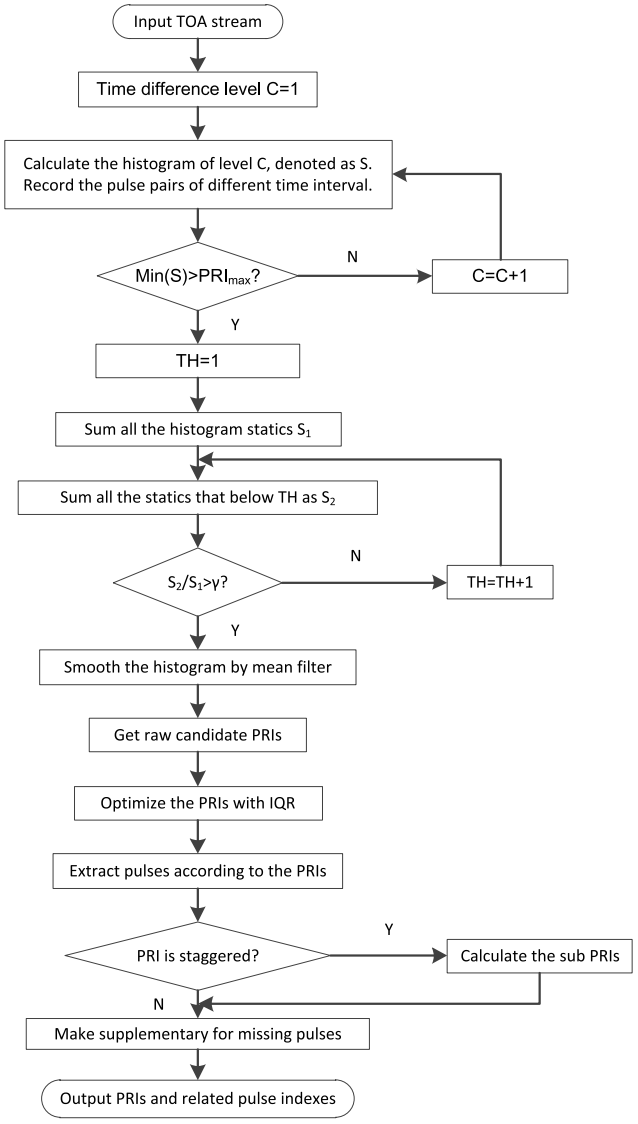

FIGURE 4. **Flow chart of PRI deinterleaving algorithm based on pulse correlation.**

extracted directly by the recorded pulse pairs as key indexes. Since the key indexes occupy the most of actual indexes, it is subtle to supplement for the missing TOAs based on key indexes. For staggered PRIs, the pulses can be sorted out by the frame period. Furthermore, the sub PRI values can be estimated by the TDOA histogram of the obtained pulses.

B. CALCULATING THE TDOA HISTOGRAM

Traditional histogram algorithms re-calculate the histogram when a candidate PRI is achieved, which leads to redundant computation. Our algorithm solve this issue by calculating the multi-level TDOA histogram, which reduces the histogram computational complexity from $\mathbf{O}(kn^2)$ to $\mathbf{O}(kn)$. k represents the level of time difference when calculating the histogram and n represents the number of pulses. The details are elaborated as a pseudo-code in Algorithm 1.

Algorithm 1 Calculation of Multi-Level TDOA Histogram

Input :
Arrival time of pulses $TOAs$;
Level of pulse time difference C;
Maximum PRI PRI_{max};
Output:
Multi-level TDOA histogram $Hist$;
Dictionary of pulse pair indexes D;

Initialize the model parameter $Hist\,[0 : PRI_{max}] = 0, C = 1, S = PRI_{max}$;
repeat
  for $i = C : L - 1$ **do**
    $\tau = TOA_i - TOA_{i-C}$;
    if $\tau < PRI_{max}$ **then**
      $Hist[\tau] = Hist[\tau] + 1$;
      $S = Min(S, \tau)$;
      $D[\tau] \leftarrow (i - C, i)$;
    end
  end
  $C = C + 1$;
until $S \leq PRI_{max}$;

In Algorithm 1, PRI_{max} is the upper limit of PRI. C is the current time difference level. $Hist$ is utilized to store the histogram statistics. D is a kind of data structure which is used to store the time differences and their corresponding pulse pairs.

Algorithm 2 Calculation of Multi-Level TDOA Histogram's Threshold

Input :
Filtered multi-level TDOA histogram $Hist_f$;
Output:
Histogram threshold TH;

Initialize the model parameter $S_1 = Sum(Hist_f), TH = 1, S2 = 0, \gamma$;
repeat
  for $\tau = 0 : PRI_{max}$ **do**
    if $Hist_f\,[\tau] < TH$ **then**
      $S_2 = S_2 + Hist_f[\tau]$;
    end
  end
  $TH = TH + 1$;
until $S_2/S_1 > \gamma$;

Before calculating the histogram threshold, the histogram should be smoothed by a mean filter, which helps to reduce the bad points. One-dimension mean filter can be expressed as:

$$Hist_f(n) = Mean\left[Hist\left(n - \frac{W-1}{2} : n + \frac{W+1}{2}\right)\right] \quad (6)$$

Here, the odd number W is window size of the filter. $Mean(\bullet)$ means calculating the average of the array. Histogram threshold is calculated based on the filtered histogram, which is introduced in Algorithm 2.

In Algorithm 2, the input is the filtered histogram and the output is the histogram threshold. γ is the key parameter for estimating the histogram threshold. As shown in Algorithm.2 and Fig.4, γ is upper limit of the ratio of S_2 to S_1, where S_1 is the sum of all the histogram statistics, and S_2 is the sum of statistics that below the threshold. When $S_2/S_1 < \gamma$, the current threshold is not big enough for estimating the candidate PRIs. On one hand, most histogram statistics of the relevant time differences are too small because they are not the PRIs. So, many fake candidate PRIs will be estimated when the γ is too small. On the other hand, some jittered PRIs will form peaks that are shorter and wider compared to the fixed PRI. So, some jittered PRIs will be ignored when the γ is too big. Since it is an experimental parameter, γ should be set according to the actual electromagnetic environment and the electronic support measure (ESM). For actual application, it is necessary to choose several values of γ to make the deinterleaving results more precious. In our simulation experiment, we test the deinterleaving *precall* with several different values of γ and set the γ to 0.3. Fig.5 is the histogram calculated based on the data simulated from Table 1. In Fig.5, the blue dotted line represents the original histogram. The green solid line is the result smoothed by the mean filter and the red line represents the threshold of the histogram. It is necessary to adopt the mean filter, since the original histogram statistics may be unstable as shown in Fig.5. These noise caused by the unstable statistics may lead to false alarm. We can eliminate these noise and achieve better raw candidate PRIs by the mean filter.

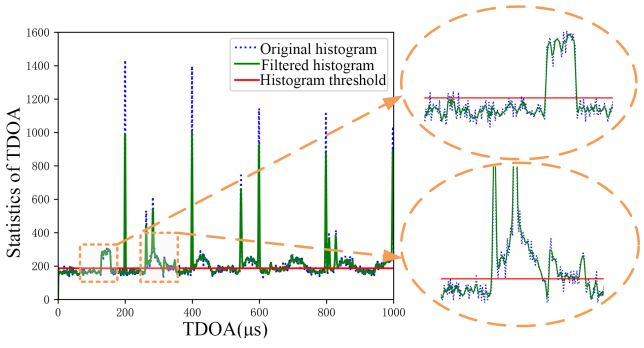

FIGURE 5. Multi-level TDOA histogram.

C. ESTIMATING THE CANDIDATE PRIs

When the filtered histogram statistics exceed the threshold, the related TDOAs are recorded as raw candidate PRIs, and they are divided into many ranges. For instance, a candidate PRI range such as $128\mu s$~$157\mu s$, or $198\mu s$~$201\mu s$. Jitter rate of fixed PRI is no more than 1%, while the jitter PRI no more than 30%. Hence, we can speculate that they may be jittered PRIs centered on $142.5\mu s$ and fixed PRIs cantered on $200\mu s$, respectively. More complicatedly, the direct correlation among pulses will lead to the failure when a fixed PRI and jittered PRI or their other combinations fall within a candidate PRI range. To search for the optimal candidate PRI centers automatically, we apply the IQR algorithm [21] to the histogram to find fliers. The fliers may come from the fixed PRIs or the staggered sub PRIs, so that we can separate the fixed PRIs from the jittered PRIs. Next, we briefly explain why the statistics of the fixed or staggered PRI histogram can be considered as fliers in boxplots. For simplicity, if two radars emit pulses with similar PRI values for the same duration, the number of pulses from the two radars will be similar too. Histogram of fixed PRI type is distributed over a narrow PRI range while a relatively wider range for the jittered type. Based on IQR, Fig.6 shows histogram boxplots of the candidate PRI ranges. The horizontal axis is TDOA range corresponding to raw candidate PRIs, and the vertical axis represents boxplots of the related histogram statistics. The height of box in the boxplots is called the IQR, and the dotted line is the median of the histogram statistics. The plus signs represent filers. We can recognize that the raw candidate PRIs in the range of $128\mu s$~$157\mu s$ and $198\mu s$~$201\mu s$ have no fliers. So they can be regarded as jittered and fixed PRI types according to the fluctuation rate. When PRI ranges from $260\mu s$ to $351\mu s$, the fliers in boxplots are related to the two peaks in Fig.5. We pick the PRIs out according to the fliers and extract pulses from the whole range. PRIs ranging from $397\mu s$ to $401\mu s$ are subharmonic of PRIs centered on around $200\mu s$. In $542\mu s$~$601\mu s$, the fliers represent the frame period of the staggered PRI. On basis of the above analysis, we can estimate the PRIs from the raw candidate PRI ranges. And the fixed and jittered PRIs are stored separately.

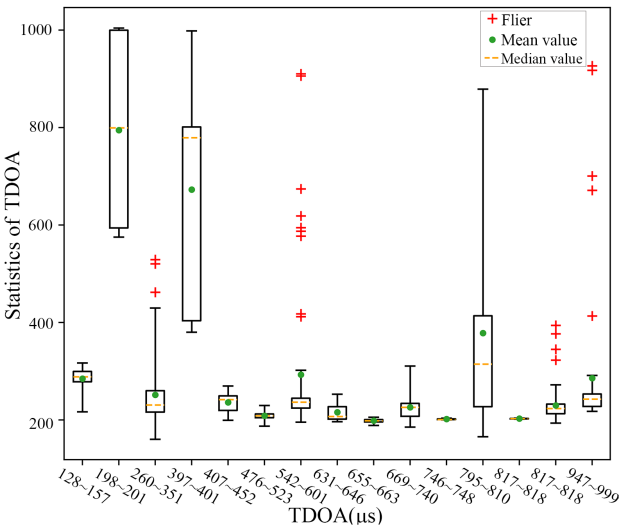

FIGURE 6. Boxplots of histogram statistics exceeding the threshold.

D. EXTRACTING PULSES AND POST PROCESSING

From the flow chart in Fig.4, we record the pulse pair indexes while calculating the histogram. The pulse pairs set of

different time difference could be expressed as bellow:

$$P_\tau = \{(m, n), \tau_L \le t_n - t_m \le \tau_H, 1 \le m < n \le L\} \quad (7)$$

Here, P_τ is the pulse pair indexes of time difference τ. τ_L, τ_H are the minimum and maximum limit of the τ, separately. We assume that all the left indexes are combined as P_L, and the right as P_R. P_L and P_R can be formulated as below:

$$g_L = \sum_{i=1}^{M} \delta\left(t - t_{m_i}\right), m_i \in P_L \quad (8)$$

$$g_R = \sum_{j=1}^{N} \delta\left(t - t_{n_j}\right), n_j \in P_R \quad (9)$$

Here, M, N are the number of left and right indexes. m_i, n_j are pulse index. The correlation of $g_L(t)$ and $g_R(t)$ is computed as:

$$R(\tau) = \int_{-\infty}^{\infty} g_L(t) g_R(t+\tau) dt = \sum_{j=1}^{N} \sum_{i=1}^{M} \delta\left(\tau - t_{n_j} + t_{m_i}\right) \quad (10)$$

Here, $R(0)$ is correlated results denoted as key indexes. When the number of extracted TOAs is small, the corresponding PRI will be recognized as sub PRI of the staggered PRI and pushed into the buffer. Taking the integrity of the TOA train into account, the process of detection and supplementary for the missing pulses is necessary.

In Fig.7, we illustrate the supplementary for the missing pulses. The green cubes are indexes gotten by correlation computing, and denoted as temporary key indexes. The red cubes are the head and tail indexes that are omitted in the temporary key indexes. The black cubes are indexes which are omitted in the middle while calculating the correlation. The white cubes are pulse indexes omitted in the original pulse train.

FIGURE 7. Schematic diagram of pulse supplementary.

Since we get the temporary key indexes, it is easy to find the head and tail indexes that do not occur in the temporary key indexes. Then we traverse the pulses among the discontinuous achieved indexes to obtain middle pulses that may be lost, calculation of which is simple. In principle, we first deal with fixed and staggered PRI types, then deal with other complex types. The only difference between fixed and jitter-like PRI types in deinterleaving is the width of PRI ranges. During the process of extracting TOA trains, it is necessary to determine whether the PRI is staggered or not. In Fig.2, PRI_1 and PRI_2 are sub PRIs, and PRI_T is sum of them. Both PRI_1 and PRI_2 get peaks in TDOA histogram. However, they are discrete correlated TOAs in time domain, and it is impossible to get key indexes by computing correlation. Fortunately, the correlated key indexes can be obtained by the PRI of PRI_T. For a fixed PRI, the number of pulses in time duration T is around $N = T/PRI$. But for a frame period of a staggered PRI type, the number of pulses in time duration T is about $N = kT/PRI$, where k is the number of sub PRIs. Considering the missing pulses, we add a ratio α to make the decision more reasonable.

$$N_s = \frac{\alpha T}{PRI} \quad (11)$$

Here, α is used to determine whether the PRI is the frame period of staggered PRIs or not. Assume that there were no pulses missed in the pulse stream, pulses of two-staggered PRIs will be twice as the pulses of fixed PRI with the same interval as the frame period. Furthermore, N-staggered PRIs will be N times, which is shown in Fig.2. Taking the pulse missing into consideration, the picked pulses will be fewer. As for two-staggered PRIs, the α should be more than one and less than two. In our simulation experiment, we conduct several supplementary experiments to test whether our method can recognize the staggered PRIs with different values of α. α is an adjustable parameter, which is set to 1.5 in this paper. If the number of extracted TOAs is beyond the N_s, the PRI can be considered as staggered. For the staggered PRI, we continue to estimate its sub PRIs by calculating the TDOA histogram from the obtained pulses.

IV. EXPERIMENTAL RESULTS

We adopt *precall* and *perror* to evaluate the performance of deinterleaving algorithms. The two indicators are defined as bellow:

$$precall = \frac{1}{n} \sum_{i=1}^{n} \frac{TP_i}{P_i} \quad (12)$$

$$perror = \frac{1}{n} \sum_{i=1}^{n} \frac{|PRI_{ei} - PRI_{ai}|}{PRI_{ai}} \quad (13)$$

Here, P_i, TP_i are the predicted and original number of pulses corresponding to the *i-th* PRI, respectively. PRI_{ei}, PRI_{ai} are estimated and actual PRI values, respectively. We compare the results with CDIF and SDIF which are PRI deinterleaving algorithms based on TDOA histogram.

A. PULSE STREAM CONSISTED OF FIXED PRIs

We design three groups of experiments. In each group, every pulse train consists of three different fixed PRIs. All the three algorithms can estimate the PRIs with *perror* less than 1e-3. We calculate the *precall* of different algorithms at variable pulse missing rates, and the results are shown in Table 2.

In Table 2, all the simulated PRIs are fixed. All of these algorithms can achieve good performance when the missing rate is small. The performances degrade as the missing rate rises. However, our algorithm shows robustness to the rising missing rate, which is mainly because our algorithm extracts pulses not based on searching.

TABLE 2. Results of pulse stream consisted of fixed PRIs.

		Algorithms				
	Missing Rate	CDIF [9]	SDIF [10]	SDIF^2 [3]	SDIF^3 [11]	Our Method
Exp.1	0	**0.997**	0.959	0.984	0.996	0.980
	0.05	0.875	0.863	0.888	**0.895**	0.890
	0.1	0.716	0.730	0.794	0.785	**0.810**
Exp.2	0	**0.998**	0.986	0.994	0.997	0.981
	0.05	0.885	0.910	**0.913**	0.912	0.891
	0.1	0.762	0.793	0.801	0.799	**0.804**
Exp.3	0	0.975	0.978	0.983	**0.989**	0.988
	0.05	0.784	0.869	0.873	0.873	**0.895**
	0.1	0.768	0.643	0.770	0.783	**0.809**

B. PULSE STREAM CONSISTED OF FIXED AND JITTERED PRIs

First, we design three groups of experiments. The simulation pulses of each group are from three emitters with different PRI values. The PRIs consist of both fixed and jittered types. We compare our algorithm with CDIF and SDIFs. The results prove that our algorithm performs better as is shown in Table 3. More pulses are extracted and the estimated PRI values are more precious.

Next, we expand the experiment to examine how the missing rate and number of emitters affect the deinterleaving results in detail. We simulate the data of three radar emitters and change the missing rate from 0 to 0.4. The *precall* of the different algorithms is shown in Fig.8. We can see that the performance of the five algorithms degrades rapidly as missing rate rises. Both CDIF and SDIFs include a searching procedure, which is dependent on the pulse integrity. Even the existing histogram methods take missing pulses into consideration, the fluctuation propagation of the PRIs will increase the error. Because our method extracts the pulses directly based on the recorded pulse pairs, the results will not be affected by the fluctuation propagation. Consequently, our method is better than CDIF and SDIFs in dealing with the pulse missing problem.

Fig.9 shows that the *precall* degrades as the number of emitters increases. It is inevitable that the deinterleaving results get worse because the the pulses extracted earlier include pulses from other emitters. Since our method extracts the pulses much more precisely from the start, the effect of the order is smaller.

To visualize the effect of pulse extracting order on the results, we plot the confusion matrix of *precall* of different methods in Fig.10. We simulate five emitters of different PRIs

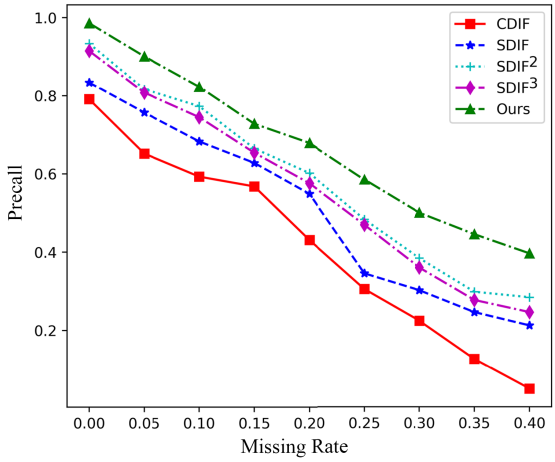

FIGURE 8. *Precall* on different missing rates.

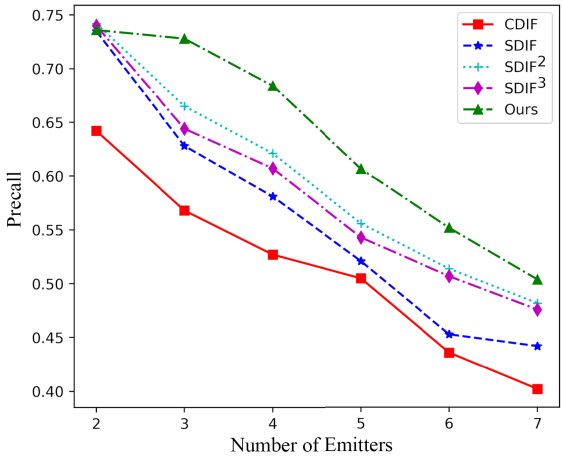

FIGURE 9. *Precall* on different number of emitters.

TABLE 3. Results of pulse stream consisted of fixed and jittered PRIs.

		Algorithms									
		CDIF [9]		SDIF [10]		SDIF^2 [3]		SDIF^3 [11]		Our Method	
	Missing Rate	*precall*	*perror*	*precall*	*perror*	*precall*	*perror*	*precall*	*perror*	*precall*	*perror*
Exp.1	0	0.869	4.8e-3	0.896	2.5e-3	0.903	2.6e-3	0.943	**2.4e-3**	**0.982**	2.6e-3
	0.05	0.656	5.4e-3	0.701	3.5e-3	0.894	3.1e-3	0.885	2.9e-3	**0.894**	**2.6e-3**
	0.1	0.579	5.9e-3	0.587	8.1e-3	0.796	4.8e-3	0.727	4.5e-3	**0.819**	**2.6e-3**
Exp.2	0	0.88	2.8e-3	0.878	3.6e-3	0.918	2.9e-3	0.906	2.8e-3	**0.957**	**2.4e-3**
	0.05	0.684	3.6e-3	0.672	5.3e-3	0.805	4.9e-3	0.812	4.7e-3	**0.881**	**2.4e-3**
	0.1	0.571	4.2e-3	0.601	6.2e-3	0.720	5.8e-3	0.732	5.5e-3	**0.814**	**2.4e-3**
Exp.3	0	0.791	3.5e-3	0.834	4.2e-3	0.934	3.8e-3	0.915	3.7e-3	**0.986**	**2.5e-3**
	0.05	0.652	5.5e-3	0.657	5.8e-3	0.817	4.5e-3	0.808	4.5e-3	**0.901**	**2.5e-3**
	0.1	0.593	7.8e-3	0.583	6.9e-3	0.773	5.8e-3	0.745	5.4e-3	**0.823**	**2.5e-3**

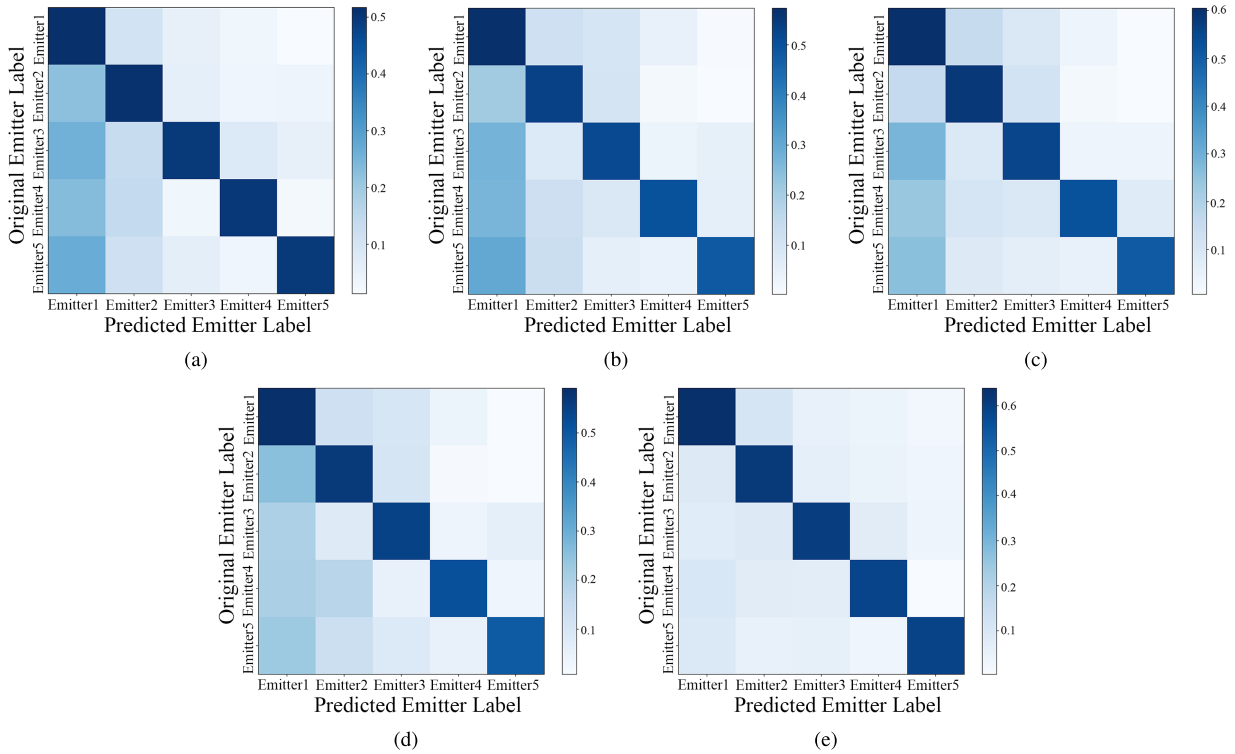

FIGURE 10. (a) *Precall* of CDIF [9]. (b) *Precall* of SDIF [10]. (c) *Precall* of SDIF^2 [3]. (d) *Precall* of SDIF^3 [11]. (e) *Precall* of Ours. (Missing rate = 0.15, Number of emitters = 5).

TABLE 4. Results of pulse stream consisted of fixed, jittered and staggered PRIs.

	Missing Rate	*precall*	*perror*	*perror* of sub PRIs
Exp.1	0	0.936	8.1e-3	1.6e-3
	0.05	0.869	9.0e-3	1.6e-3
	0.1	0.754	9.1e-3	1.6e-3
Exp.2	0	0.935	8.0e-3	2.0e-3
	0.05	0.869	8.5e-3	2.0e-3
	0.1	0.810	9.7e-3	2.0e-3
Exp.3	0	0.947	7.7e-3	1.8e-3
	0.05	0.878	8.5e-3	1.8e-3
	0.1	0.791	9.6e-3	1.8e-3

at the missing rate 0.15. In Fig.10, the deeper the blue is, the higher the *precall* will be. We number the emitters according to the order in which the pulses are extracted. As for our method, the deinterleaving results of each emitter are much more precise compared to CDIF and SDIFs algorithm.

In conclusion, the searching procedure of the traditional histogram methods is straightforward but inappropriate. When the searching base pulse is not precise, the error of TOAs will propagate. Our method based on pulse correlation performs better.

C. PULSE STREAM CONSISTED OF FIXED, JITTERED, STAGGERED PRIs

Here, three groups of experiments are designed. Each group contains 4 emitters with different PRIs, including the fixed, jittered and staggered PRIs. Since CDIF and SDIFs do not take the staggered PRIs into consideration, our algorithm will not be compared with them. In Table 4, we evaluate the algorithm by *precall* and *perror*. Also, the *perror* of sub PRIs is calculated. Table 4 shows that our algorithm can extract most of the pulses out and estimate the sub PRI values as well.

V. CONCLUSION

In this paper, we first calculate the multi-level TDOA histogram, and record the pulse pair indexes at the same time. Then we adopt a mean filter for the histogram and calculate the threshold for the filtered histogram. Raw PRI ranges are obtained after comparing the filtered histogram with threshold. We utilize IQR algorithm to split the fliers out when the fixed and jittered PRIs are overlapped in the TDOA histogram. TOAs can be extracted based on the recorded pulse pair indexes directly. At last, the staggered checking and supplementary will be added.From the experimental results, we can see that our algorithm can extract more pulses accurately and estimate the PRI values more preciously. Our method shows robustness to the jitter rate, missing rate and the number of radar emitters. Also, our algorithm can estimate the sub PRIs for the staggered PRIs.

REFERENCES

[1] P. M. Grant and J. H. Collins, "Introduction to electronic warfare," *IEE Proc. F-Commun. Radar Signal Process.*, vol. 129, no. 3, pp. 113–132, Jun. 1982.

[2] P. W. East and J. L. Everett, "Electronic support measures," *IEE Proc. F Commun., Radar Signal Process.*, vol. 132, no. 4, p. 205, Jul. 1985.
[3] Y. Liu and Q. Zhang, "An improved method for deinterleaving radar signals and estimating PRI values," *IET Radar, Sonar Navigat.*, vol. 12, no. 5, pp. 506–514, 2018.
[4] C. Li, "The research of radar signal sorting technology," M.S. thesis, Univ. Electron. Sci. Technol. China, Chengdu, China, 2015.
[5] H. E. Hassan, "Deinterleaving of radar pulses in a dense emitter environment," in *Proc. Int. Radar Conf.*, Adelaide, SA, Australia, Sep. 2003, pp. 389–393.
[6] J. A. V. Rogers, "ESM processor system for high pulse density radar environments," *IEE Proc. F Commun., Radar Signal Process.*, vol. 132, no. 7, pp. 621–625, Dec. 1985.
[7] J. B. Moore and V. Krishnamurthy, "Deinterleaving pulse trains using discrete-time stochastic dynamic-linear models," *IEEE Trans. Signal Process.*, vol. 42, no. 11, pp. 3092–3103, Nov. 1994.
[8] C. Zhao and G. Zhao, "An improved algorithm for the deinterleaving of radar signals based on stochastic dynamic linear models," *Syst. Eng. Electron.*, vol. 25, no. 9, pp. 1049–1051, 2003.
[9] H. K. Mardia, "New techniques for the deinterleaving of repetitive sequences," *IEE Proc. F Radar Signal Process.*, vol. 136, no. 4, pp. 149–154, Aug. 1989.
[10] D. J. Milojević and B. M. Popović, "Improved algorithm for the deinterleaving of radar pulses," *IEE Proc. F (Radar Signal Process.)*, vol. 139, no. 1, pp. 98–104, 1992.
[11] Y. Xi, Y. Wu, X. Wu, and K. Jiang, "An improved SDIF algorithm for anti-radiation radar using dynamic sequence search," in *Proc. Chin. Control Conf.*, Dalian, China, Jul. 2017, pp. 5596–5601.
[12] K. Nishiguchi and K. Masaaki, "Improved algorithm for estimating pulse repetition intervals," *IEEE Trans. Aerosp. Electron. Syst.*, vol. 36, no. 2, pp. 407–421, Apr. 2000.
[13] Y. Mao *et al.*, "An improved algorithm of PRI transform," in *Proc. WRI Global Congr. Intell. Syst.*, vol. 3, 2009, pp. 145–149. [Online]. Available: https://ieeexplore.ieee.org/document/5209181
[14] A. Mahdavi and A. M. Pezeshk, "A fast enhanced algorithm of PRI transform," in *Proc. Int. Symp. Parallel Comput. Elect. Eng.*, Hefei, China, Oct. 2011, pp. 179–184.
[15] G. Quan, Y. Sun, and B. Chen, "Folding deinterleaving algorithm for multiple mixed pulse trains with pulse repetition intervals," in *Proc. Int. Conf. Mach. Learn. Cybern.*, Dalian, China, Aug. 2006, pp. 3334–3338.
[16] A. W. Ata'a and S. N. Abdullah. "Deinterleaving of radar signals and PRF identification algorithms," *IET Radar, Sonar Navigat.*, vol. 1, no. 5, pp. 340–347, 2007.
[17] T. Li, D.-W. Feng, and W. L. Jiang, "Radar pulse PRF deinterleaving algorithm based on pulses' relativity," *Electron. Inf. Warfare Technol.*, vol. 22, no. 1, pp. 10–13, 2007.
[18] W.-J. Ren, D.-H. Hu, and C.-B. Ding, "Multi-TDOA location algorithm for three satellites TDOA passive location system," *J. Radars*, vol. 1, no. 3, pp. 262–269, 2012.
[19] G. Xie, H.-X. Wang, Z. Xu, and W. Chao, "A fast sorting method for modulated and jitter PRI radar signals," in *Proc. Int. Conf. Transp.*, Changchun, China, Dec. 2012, pp. 2210–2213.
[20] Y. Yu, X. Zhang, and K. Li, "A jittered signal sorting algorithm based on cumulative square sine wave interpolation," *Radar ECM*, vol. 33, no. 1, pp. 12–16, 2013.
[21] H. Jiawei, *Data Mining: Concepts and Techniques*. San Mateo, CA, USA: Morgan Kaufmann, 2005.

ZHIPENG GE (S'19) received the B.Sc. degree from the Ocean University of China, Qingdao, China, in 2016. He is currently pursuing the M.S. degree with the Institute of Electronics, Chinese Academy of Sciences, Beijing, China.

His research interests include signal processing, computer vision, and pattern recognition, especially on radar deinterleaving.

XIAN SUN received the B.Sc. degree from the Beijing University of Aeronautics and Astronautics, Beijing, China, in 2004, and the M.Sc. and Ph.D. degrees from the Institute of Electronics, Chinese Academy of Sciences, Beijing, in 2009.

He is currently a Professor with the Institute of Electronics, Chinese Academy of Sciences. His research interests include computer vision and remote sensing image understanding.

WENJUAN REN received the B.Sc. degree from Xidian University, Xi'an, China, in 2005, and the M.Sc. and Ph.D. degrees from the Institute of Electronics, Chinese Academy of Sciences, Beijing, in 2011.

She is currently an Associate Professor with the Institute of Electronics, Chinese Academy of Sciences. Her research interests include signal processing, radar technology, communication engineering, and data mining.

WENBIN CHEN received the B.Sc. degree from Tianjin University, Tianjin, China, in 2014. He is currently pursuing the Ph.D. degree with the Institute of Electronics, Chinese Academy of Sciences, Beijing, China.

His research interests include signal processing and machine learning, especially on radar recognition.

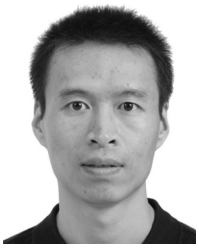

GUANGLUAN XU received the B.Sc. degree from Peking University, Beijing, China, in 2000, and the M.Sc. and Ph.D. degrees from the Institute of Electronics, Chinese Academy of Sciences, Beijing, in 2005, where he is currently an Associate Professor. His research interests include computer vision and geospatial information application technology.